Active flow control of a 2:1 rectangular jet using dielectric barrier discharge plasma actuators

Naoki KAJITANI[1*], Takumi MATSUO[1], Peter OSHKAI [2] and Takahiro KIWATA[3]

1: Graduate School of Natural Science and Technology, Kanazawa University, Kakuma-machi, Kanazawa-shi, Ishikawa, Japan
2: Department of Mechanical Engineering, University of Victoria, 3800 Finnerty Road, Victoria, BC, Canada
3: School of Mechanical Engineering, Kanazawa University, Kakuma-machi, Kanazawa-shi, Ishikawa, Japan

* Correspondent author: n.kajitani@stu.kanazawa-u.ac.jp

Abstract

The purpose of the present study is to establish an active flow control method for a 2:1 rectangular jet using DBD plasma actuators installed at a nozzle exit. The Reynolds number of the rectangular jet is $Re = 9.0\times10^3$. The PAs were supplied with an AC sinusoidal high-voltage waveform, i.e. a voltage E = 10 kVp-p and a frequency f_b = 10 kHz. The pulse frequency f_p (= $1/T$) was varied at 86 Hz, which was the natural vortex frequency of a rectangular jet, and 172 Hz. The duty ratio D_u (=T_{ON}/T, T_{ON}: voltage input time during one cycle) was also varied from 0.1 to 1. The flow characteristics of a rectangular jet can be controlled by the variation of the pulse frequency f_p and duty ratio D_u of the DBD plasma actuators which are installed on the tip of the nozzle's long side.

Keywords: *DBD plasma actuator, Rectangular jet, Flow control, Flow visualization, PIV*

1. Introduction

Free jets injected from a rectangular nozzle into a static fluid have been used in applications, for example, air curtains of showcases, and air conditioning systems. As the vortex behavior has a great influence on flow characteristics of mixing, diffusion, and noise in the jet, many studies have been conducted to control the flow of a jet by externally perturbing the vortices formed in the free shear layer. Recently, there has been increasing interest in dielectric barrier discharge (DBD) plasma actuators (PAs) for flow control. This device has very attractive features such as lightweight, low power consumption, fast response time, and no mechanical moving parts. Due to their effectiveness, PAs have been studied in numerous applications, including boundary layer flow control, prevention of icing on aircraft and wind turbines, and control of buffeting noise [1]-[3]. Kozato et al. [4] and Pham et al. [5] showed that the spread of a rectangular jet with a large aspect ratio can be controlled by varying the pulse frequency using PAs on the long sides of the nozzle. Prasad et al. also performed a computational study on the effects of localized arc filament plasma actuators based control on the flow field and acoustics of a supersonic 2:1 aspect ratio rectangular jet [6].

The purpose of the present study is to establish an active flow control method for a 2:1 aspect ratio rectangular jet using DBD plasma actuators installed at a nozzle exit. We will experimentally investigate the effects of varying the pulse frequency and the duty ratio of the applied voltage waveform on the flow characteristics of a rectangular jet by installing PAs on the long side of the nozzle of a rectangular jet with a relatively low Reynolds number.

2. Experimental Apparatus and Method

Experiments were conducted using a blow-down wind tunnel with a rectangular nozzle, which had a contraction with dimension reduction ratios of 2.8:1. Figure 1 shows the schematic diagram of the rectangular nozzle with DBD-PAs. The rectangular nozzle had a height H of 30 mm and a width B of 60 mm, that is an aspect ratio of 2. The velocity U_0 of the jet was adjusted to $U_0 \approx 4.5$ m/s at the center of the nozzle exit. The

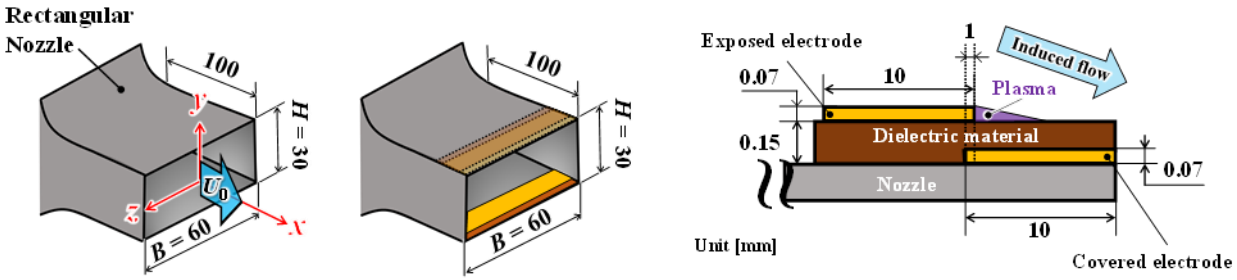

(a) Without PAs (b) PAs added to long sides of rectangular nozzle (c) Cross-sectional view of a PA

Fig.1 Schematic diagram of the rectangular nozzle with DBD-PAs

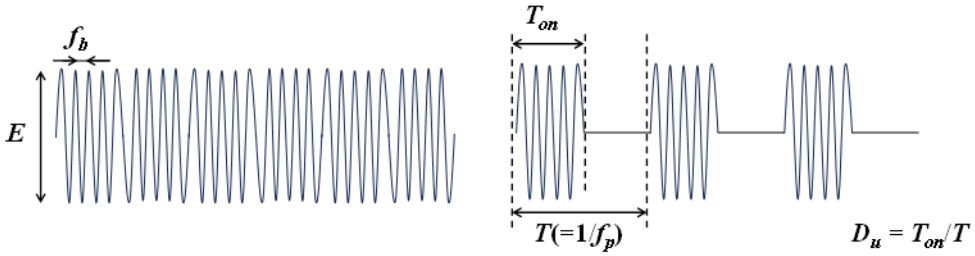

(a) Continuous operation (b) Pulsed operation

Fig.2 Input waveform to the DBD-PAs

Reynolds number is Re ($=U_0H/\nu$, where ν: kinematic viscosity of air) = 9.0×10^3. The x-axis was the streamwise direction of the jet, and the y-axis and z-axis were the spanwise directions along the nozzle's short and long sides, respectively.

PAs were installed on the tip of the nozzle's long side. PAs were composed of an exposed electrode, an electrode covered in copper, and three layers of dielectric material made of a polyamide. The PAs were supplied with an AC sinusoidal high-voltage waveform, i.e. a voltage E = 10 kVp-p and a frequency f_b = 10 kHz, by the high-voltage pulse power supply unit (Powers System Integrate Ltd., PSI-PA1050N, PSI-PW0500, and PSI-TR10). The AC wave signal is provided to the high-voltage pulse power supply unit by an arbitrary function generator (TEXIO Technology Co., FGX-2220). The pulse frequency f_p (= $1/T$) was varied at 86 Hz, which was the natural vortex frequency of a rectangular jet, and 172 Hz. The duty ratio D_u ($=T_{ON}/T$, T_{ON}: voltage input time during one cycle) was also varied from 10 % to 100 %.

The flow fields of the rectangular jets were measured using the particle image velocimetry (PIV) system. Continuous images for 30 seconds and 240 pairs were acquired at a frame frequency of 8 Hz and pixel resolution of 2,448 × 2,058 with a CCD camera (DANTEC Dynamic, FlowSense EO 5M) and processed by the commercially available DANTEC Dynamic Studio Ver. 6.9 software suite. A double-pulse Nd:YAG laser (DANTEC Dynamic, Dual Power 200-15, 200 mJ) was used to produce light sheets in the x-y, x-z, and y-z planes. The size of the interrogation window was 340 mm and 400 mm in the vertical and horizontal directions, respectively. A fog generator (SAFEX Fog Generator) was used to produce an oil mist to provide tracer particles with mean diameters of approximately 1 μm. The particle fluid density was 1,030 kg/m^3. The PIV system was also employed for the visualization of vortical structures in the rectangular jets. The spatial density of particles in the flow visualization working fluid was much larger than that used for the PIV system velocity measurements.

3. Experimental Results and Discussion

3.1 Instantaneous flow visualization of a rectangular jet

Figure 3 shows the instantaneous flow visualization images in the x-y cross-section at z/H = 0, the x-z cross-section at y/H = 0, and the y-z cross-section at x/H = 1. In the case of a jet without PAs (Fig.3(a)), the roll-up of the large-scale vortices can be seen in the shear layers at $x/H > 2$ in the x-y and the x-z cross-sections. These large-scale vortical structures collapse into small-scale vortical structures in the downstream region, and the

jet spreads significantly. In the *y*-*z* cross-section, the outline of a rectangular jet is maintained due to the potential core region. In the case of continuous operation of the PAs that were installed at the tip of the long side of the nozzle (Fig.3(b)), the relatively small-scale vortices are generated in the shear layers, starting at the exit of the nozzle. As a result, the jet doesn't spread in the *x*-*y* cross-section, in contrast to the jet without the PAs. In the *x*-*z* cross-section, the large-scale vortices can be seen around $x/H \approx 2$, similar to the jet without the PAs. In the *y*-*z* cross-section, streamwise vortices can be observed on the long side of the nozzle, i.e. on the side of PAs. In the case of the pulse frequency of f_p = 86 Hz and the duty ratio of Du = 10% (Fig.3(c)), large-scale vortices are generated in the *x*-*y* cross-section near the nozzle at $x/H \approx 0.5$. Due to the vortex pairing phenomenon, the jet spread increases in downstream, compared to Fig. 3(a) and (b). In the *y*-*z* cross-section, the spanwise and the streamwise vortices are generated in the shear layers, and the cross-sectional shape of the

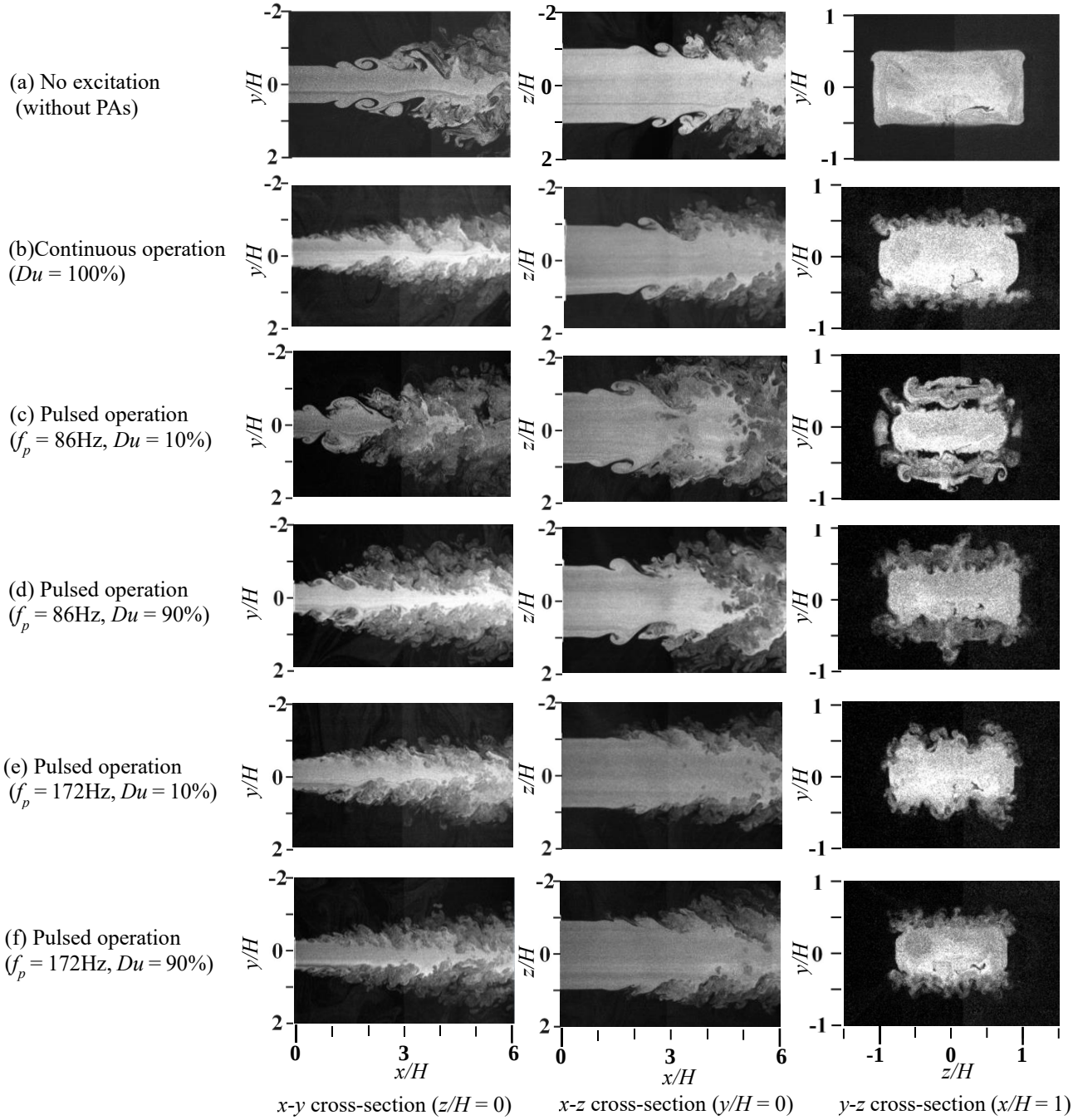

Fig.3 Instantaneous flow visualization images of a 2:1 rectangular jet excited by DBD-PAs on the tip of the nozzle's long side

jet differs from the cases of no excitation (Fig. 3(a)) and of continuous actuation (Fig. 3(b)). In the case of f_p = 86 Hz and D_u = 90% (Fig. 3(d)), large-scale vortices are also generated in the *x*-*y* cross-sections near the nozzle at $x/H \approx 0.5$. However, these vortices changed to small-scale vortices, in contrast to the case of Du = 10% (Fig.3(c)). The flow patterns in the *x*-*z* and the *y*-*z* cross-sections are similar to that of the case of continuous driving of the PAs (Fig. 3(b)). In the case of f_p = 172 Hz (Fig. 3(e) and (f)), relatively small-scale vortices are generated in the shear layers near the nozzle in the *x*-*y* cross-section. The jet spread is also similar to the case of D_u = 90% (Fig. 3(e)). Therefore, the effect of change in the duty ratio D_u on the jet spread decreases with the increasing the pulse frequency f_p. However, in the *y*-*z* cross-section, the large distortion of the jet outline is observed for D_u =10%.

3.2 Contours of time-averaged streamwise velocity in the *x*-*y* cross-section

Figure 4 shows the contour distribution of the time-averaged streamwise velocity $\overline{u}/U_0$ in the *x*-*y* cross-section. First, without PAs in Fig. 4(a), the jet spreads significantly in the ±*y* directions from $x/H \approx 3$ corresponding to the large-scale vortex formation, as shown in Fig. 3(a). In the downstream region at $x/H > 6$, the potential core region (red color) disappears as the jet velocity decays. In the case of continuous operation in Fig. 4(b), the jet spreads linearly in the ±*y* directions immediately after an air ejection from the nozzle due to the generation of small-scale vortices near the nozzle outlet, as shown in Fig. 3(b). As a result, the jet spread is smaller up to x/H = 12 compared to without PAs in Fig. 4(a). The rectangular jet with f_p = 86Hz and a duty ratio D_u = 10% in Fig. 4(c) spreads out from near the nozzle exit due to the generated large-scale vortices in the *x*-*y* cross-section, as shown in Fig. 3(c). This behavior differs significantly from that without PAs as shown in Fig. 4(a), and that for the continuous operation as shown in Fig. 4(b). The spread of a rectangular jet with PAs operated for f_p = 86 Hz and D_u = 90% in Fig. 4(c) is smaller compared to that for D_u = 10% (Fig.4(c)) because small-scale vortices are generated in the shear layer as shown in Fig. 3(d). On the other hand, the rectangular jet with f_p = 172Hz and D_u = 10% in Fig. 4(e) shows a smaller spread compared to the rectangular jet without PAs and with f_p = 86 Hz pulsed drive. This behavior is due to the suppression of large-scale vortex generation by small-scale vortex generation and is similar to that of the continuous operation in Fig. 4(b). In Fig. 4(f), for f_p = 172Hz and D_u = 90%, the rectangular jet spreads linearly from near the nozzle exit and is almost the same as without PAs in Fig.4(a). However, there is a large velocity region (red color) that maintains up to $x/H \approx 10$.

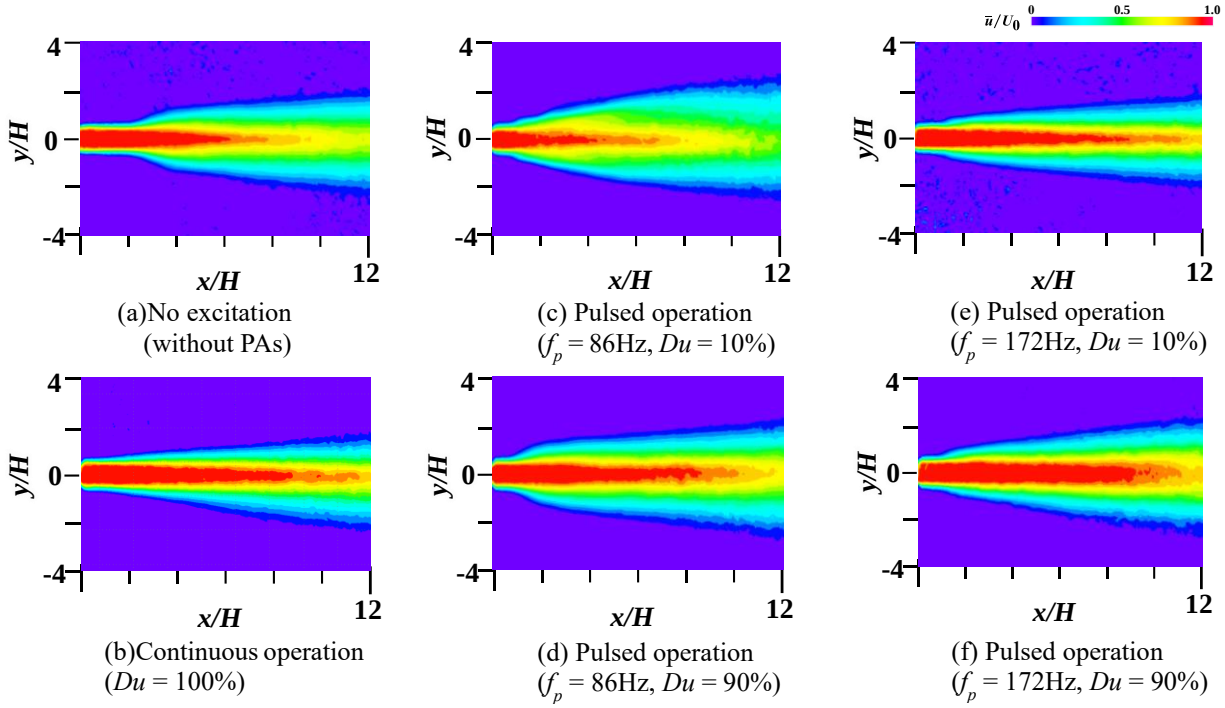

Fig.4 Contours of time-averaged streamwise velocity of a 2:1 rectangular jet excited by DBD-PAs on the tip of the nozzle's long side

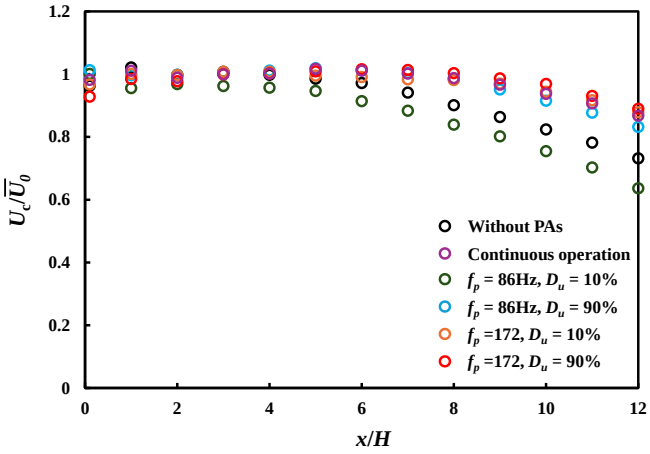

Fig.5 Profiles of the time-averaged streamwise velocity along the jet centreline

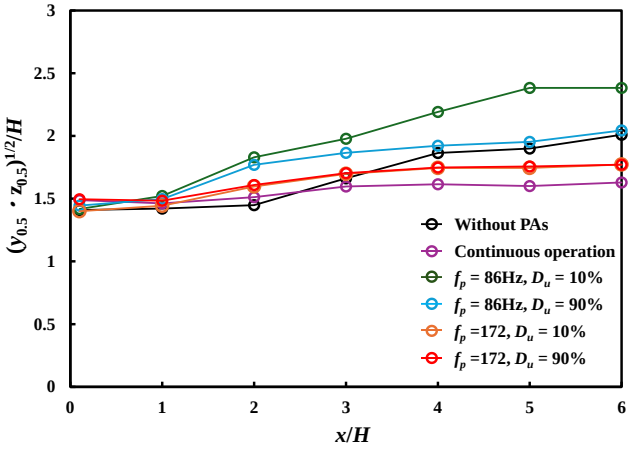

Fig.6 Variations of equivalent jet half velocity width

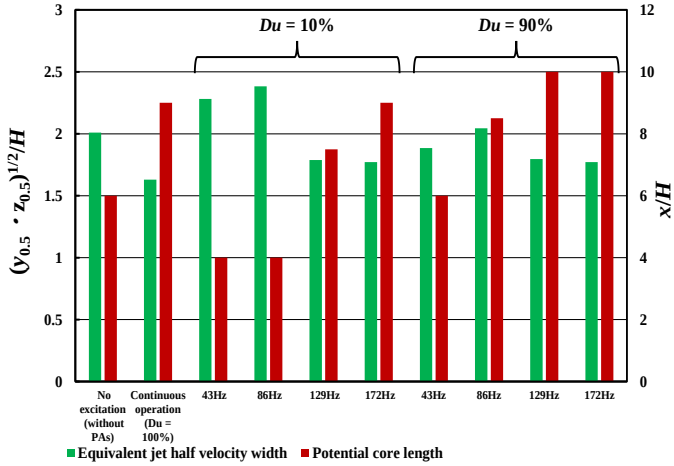

Fig.7 Effect of pulse frequency f_p on equivalent jet half velocity width and potential core length

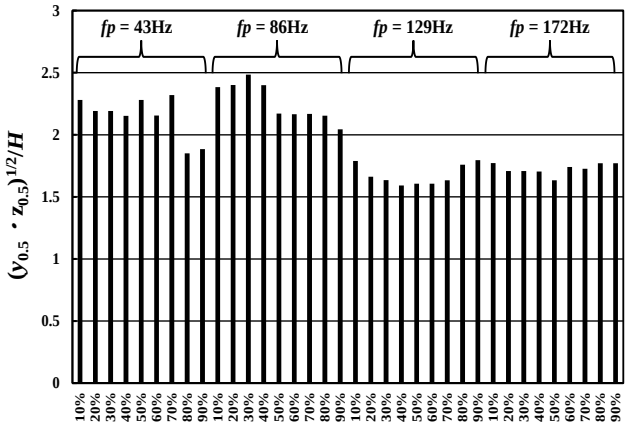

Fig.8 Effect of duty ratio *Du* on equivalent jet half velocity width

3.3 Centerline velocity and Equivalent jet half velocity width

Figure 5 shows the time-averaged streamwise velocity $\overline{u_c}/U_0$ along the jet centerline. The potential core length is defined as the distance between the nozzle exit and the point in x-direction where the centerline velocity decays to 95% of the velocity at the nozzle exit. The potential core lengths of the rectangular jet without PAs, and with PAs for the continuous operation and pulsed operation at (f_p, D_u) = (86Hz, 10%), (86Hz, 90%), (172Hz, 10%), and (172Hz, 90%) are approximately 6H, 9H, 4H, 8.5H, 9H, and 10H, respectively. The potential core region of the rectangular jet with PAs pulsed at f_p = 86Hz and D_u = 10% is smaller and more pronounced velocity decay downstream than the other jets. On the other hand, the potential core length of the rectangular jet with PAs for continuous operation is larger than that with PAs pulsed operation at f_p = 86Hz. The velocity distribution along the jet centerline for the rectangular jet with PAs for the continuous operation is almost similar to those of pulsed operation at f_p = 172Hz. The rectangular jet with the pulsed operation at f_p = 129, 172Hz and D_u = 90% has the longest potential core length. These behaviors are related to vortex structures as shown in Fig. 3.

Figure 6 shows the equivalent jet spread [4], i.e., the equivalent jet half velocity width $(y_{1/2} \cdot z_{1/2})^{0.5}/H$, along the x-axis normalized by the nozzle height, where $y_{1/2}$ and $z_{1/2}$ are the half-velocity width of the rectangular jet in the x-y and x-z cross-sections, respectively. The jet half-velocity width is defined as the point in the y- or z-direction where the velocity drops to half the maximum velocity, i.e., the centerline velocity. The equivalent jet spread signifies the overall spread of the rectangular jet along the x-axis. The rectangular jet with PAs for f_p = 86Hz and D_u = 10% has the largest equivalent jet spread compared to the other jets and this jet velocity decays significantly. This result is understood by the flow structure in Fig. 3(c) and the velocity distribution in Fig. 4(c). On the other hand, the smallest equivalent jet spread at x/H = 6 was observed for the rectangular jet with PAs of continuous operation. For rectangular jets with PAs of pulse operated at f_p = 172Hz, the equivalent

jet spread at $x/H \leqq 3$ was almost same as for continuous operation (D_u = 100%). Therefore, the pulsed operation of PAs is also effective enough to control the jet spread from the viewpoint of power consumption.

Figure 7 shows the comparison of the equivalent jet half velocity width (x/H = 6) and the potential core lengths with pulse frequencies f_p varied from 43Hz to 172 Hz at duty ratios D_u = 10% and 90%. In the case of D_u = 10% and f_p = 43 and 86 Hz, the equivalent jet spreads tend to be larger than the other cases. In addition, the potential core length becomes short and the decay of the central linear velocity becomes fast. For D_u = 10%, and f_p = 126 and 172 Hz, the equivalent jet spread becomes smaller and the potential core becomes longer compared to f_p = 43, and 86 Hz. On the other hand, for D_u = 90%, and f_p = 43 and 86 Hz, the equivalent jet spread becomes smaller and the potential core length becomes longer than those for D_u = 10%. In particular, at f_p = 86 Hz, the potential core length doubles from 4H to 8H for D_u = 10%, and the centerline velocity almost is maintained the same as that of the continuous operation. For D_u = 90%, and f_p = 129 and 172 Hz, the equivalent jet spreads are almost the same as for D_u = 10% (f_p = 129 and 172 Hz). However, the potential core length is further increased, which is longer than that for the continuous operation. This indicates that the velocity reach of the jet can be increased with less power consumption.

Figure 8 shows the equivalent jet half velocity width (x/H = 6) varied from D_u = 10% to 90%. For f_p = 43 and 86 Hz, the equivalent jet spread tends to decrease with increasing D_u. On the other hand, for relatively high f_p of 129 and 172 Hz, the effect of the duty ratio D_u on the jet spread is smaller than that for f_p = 43 and 86 Hz.

From the above results, it can be concluded that the flow characteristics of a rectangular jet can be controlled by the variation of the pulse frequency f_p and the duty ratio D_u of the DBD plasma actuators which are installed on the tip of the nozzle's long side.

4. Conclusions

The flow characteristics of a rectangular jet operated by DBD plasma actuators installed on the long sides of a nozzle exit with an aspect ratio of 2 were experimentally investigated and the following results were obtained.

(1) The rectangular jet with PAs operated in pulses at a pulse frequency f_p = 86 Hz has a larger spread than that without PAs, due to the generation of large-scale vortices in the shear layer from near the nozzle exit. In particular, the centerline velocity of the rectangular jet for a duty ratio D_u = 10% decays faster compared to the other jets.

(2) In the case of the rectangular jet with PAs operated in pulses at f_p = 172 Hz, the equivalent jet half-velocity width is smaller and the potential core length increases more than that without PAs due to the generation of small-scale vortices in the shear layer from near the nozzle exit. There is almost no difference in the centerline velocity decay and the equivalent jet half-velocity width between D_u = 10% and 90%.

(3) The flow characteristics of a rectangular jet with a continuous operation of PAs and with a pulsed operation of PAs at f_p = 172 Hz are relatively similar. Therefore, for the flow control of a 2:1 aspect ratio rectangular jet, the pulsed operation of PAs with less power consumption is better than a continuous operation of PAs.

References

[1] Hoda Mahdavi, "An experimental investigation of the unsteady counter-flow generated by a DBD plasma actuator for flow control", The European Physical Plus, 2024 Vol.139, Article number 550, (2024), https://doi.org/10.1140/epjp/s13360-024-05341-6

[2] Jinsheng Cai, Yongqiang Tian, Xuanshi Meng, "An experimental study of icing control using DBD plasma actuator", Experiments in Fluids, Vol.58, Article number 102, (2017), https://doi.org/10.1007/s00348-017-2378-y

[3] Xingjun Hu, Hongyang Liang, Yanghui Zhang, Jingyu Wang, Peng Guo, "Active control of cavity buffeting noise using a dielectric barrier discharge plasma actuator", Mechanical Systems and Signal Processing, Vol.208, (2024), https://doi.org/10.1016/j.ymssp.2023.110959

[4] Kozato, Y., Kikuchi, S., Imao, S., Kato, Y. and Okayama, K., "Flow control of a rectangular jet by DBD plasma actuators", International Journal of Heat and Fluid Flow, Vol. 62 (2016), pp.33-43, https://doi.org/10.1016/j.ijheatfluidflow.2016.09.014

[5] Pham, A. V., Inaba, K., Saito, M. and Sakai, M., "Effect of plasma actuator on velocity and temperature profiles of high aspect ratio rectangular jet", Fluids, Vol.7 (2022), 20pages, https://doi.org/10.2139/ssrn.4069229

[6] Prasad, A.L.N., and Unnikrishnan, S., "Effect of plasma actuator-based control on flow-field and acoustics of supersonic rectangular jets", Journal of Fluid Mechanics, Vol.964, A11 (2023), https://doi.org/10.1017/jfm.2023.354

[7] Srinivasan, K. and Rathakrishnan, E., "Studies on polygonal slot jets", AIAA Journal, Vol. 38 (1985), No.10, pp. 187-196, https://doi.org/10.2514/2.855